Controllability and Optimal Strokes for N-link Micro-swimmer

Laetitia Giraldi, Pierre Martinon, Marta Zoppello

▶ **To cite this version:**

Laetitia Giraldi, Pierre Martinon, Marta Zoppello. Controllability and Optimal Strokes for N-link Micro-swimmer. 52nd IEEE Conference on Decision and Control, Dec 2013, Firenze, Italy. 10.1109/CDC.2013.6760480 . hal-00798363v3

HAL Id: hal-00798363
https://hal.science/hal-00798363v3

Submitted on 27 Apr 2016

HAL is a multi-disciplinary open access archive for the deposit and dissemination of scientific research documents, whether they are published or not. The documents may come from teaching and research institutions in France or abroad, or from public or private research centers.

L'archive ouverte pluridisciplinaire **HAL**, est destinée au dépôt et à la diffusion de documents scientifiques de niveau recherche, publiés ou non, émanant des établissements d'enseignement et de recherche français ou étrangers, des laboratoires publics ou privés.

Controllability and Optimal Strokes for N-link Microswimmer*

Laetitia Giraldi[1], Pierre Martinon[1] and Marta Zoppello[2]

***Abstract*— In this paper we focus on the N-link swimmer [1], a generalization of the classical 3-link Purcell swimmer [18]. We use the Resistive Force Theory to express the equation of motion in a fluid with a low Reynolds number, see for instance [12]. We prove that the swimmer is controllable in the whole plane for $N \geq 3$ and for almost every set of stick lengths. As a direct result, there exists an optimal swimming strategy to reach a desired configuration in minimum time. Numerical experiments for $N = 3$ (Purcell swimmer) suggest that the optimal strategy is periodic, namely a sequence of identical strokes. Our results indicate that this candidate for an optimal stroke indeed gives a better displacement speed than the classical Purcell stroke.**

I. INTRODUCTION

A. Locomotion at low Reynolds Number

Swimming at a micro scale is a subject of growing interest, with potential applications for example in medicine or micro and nano technology. The swimming strategy of micro-organisms in low Reynolds number fluids is attracting increasing attention in the recent literature, see for instance [14] for an extensive list of references. One of the pioneering works is probably [20] by Taylor in 1951, presenting a model of swimmer as an infinite sheet shaped as a sinusoidal traveling wave, with a mathematical setting for the self-propulsion of this thin undulating filament. Later in 1977, Purcell proved in [18] that the swimming strategies must change the shape of the swimmer in a non-reciprocal way, in order to permit a displacement through the fluid, and introduced a 3-link swimmer model along with a stroke that allows it to move. More recently, several works have studied in more detail the physical characteristic of this "Purcell swimmer", see for instance [19],[6],[1],[17]. Another crucial development for our analysis is the recent emergence of the connection between swimming and Control Theory ([16],[3],[4],[8],[15],[2]). One of the difficulties is the study of the swimmer-fluid coupling which gives the dynamics of the swimmer. At a micro scale, the non local hydrodynamic forces exerted by the fluid on the swimmer can be approximated with local drag forces depending linearly on the velocity of each point (see [12],[10]). This technique called Resistive Force Theory provides a simplified dynamics that matches well those obtained by the full hydrodynamic model, see [1],[10]. We use here this technique for the N-link swimmer, as in [1].

B. Contribution

In this paper, we present a controllability result for the N-link swimmer, and numerical simulations that suggest a new optimal stroke for displacement in minimum time. First, we prove by geometric control techniques that for $N \geq 3$ sticks, the N-link swimmer can reach any configuration in the plane. More precisely, we show that for almost any swimmer (i.e. for almost every set of stick lengths) and for any initial configuration, the swimmer can reach any shape and position. This result shows the existence of a suitable shape deformation which steers the swimmer to the desired final state. As a direct consequence, we show that the optimal control problem to reach a configuration in minimum time is well posed. Therefore, there exists an optimal strategy leading to the final position and configuration in minimum time. Finally, we present some numerical simulations for the Purcell swimmer ($N = 3$) with a direct method (BOCOP[1]). Without making any assumptions on the structure of the optimal strategy, our results suggest that the optimal swimming motion is indeed periodic, with a sequence of identical strokes. We observe that the stroke we obtain is different from the Purcell one, and gives a speed greater by about 15%.

II. SETTING OF THE PROBLEM

We recall the N-link swimmer introduced in [1], and present its motion as a system of three ODEs. The system is linear with respect to the deformation rate, and has no drift.

A. The N-link swimmer

The swimmer consists of $N \in \mathbf{N}$ rigid links with joints at their ends, see Fig. 1. Motion is expressed in the laboratory-frame, defined by the vectors $(\mathbf{e}_x, \mathbf{e}_y)$. We set $\mathbf{e}_z := \mathbf{e}_x \times \mathbf{e}_y$. The i-th link is the segment with end points $\mathbf{x}_i$ and $\mathbf{x}_{i+1}$. We note $L_i > 0$ its length and θ_i its angle with the horizontal x-axis. We define (x_i, y_i) the coordinates of each point $\mathbf{x}_i$ For $i \in \{2 \cdots N\}$, the coordinates $\mathbf{x}_i$ can be expressed as:

$$\mathbf{x}_i := \mathbf{x}_1 + \sum_{k=1}^{i-1} L_k \begin{pmatrix} \cos(\theta_k) \\ \sin(\theta_k) \end{pmatrix}. \tag{1}$$

The swimmer is described by two sets of variables:

- the position and orientation of the first link, associated with the triplet $(\mathbf{x}_1 = (x_1, y_1), \theta_1)$.

*This work has been partially supported by the Direction Générale de l'Armement (DGA).

[1]Centre de Mathématiques Appliquée de l'Ecole Polytechnique, CMAP UMR 7641 Ecole Polytechnique CNRS, Route de Saclay, 91128 Palaiseau, giraldi at cmap.polytechnique.fr, pierre.martinon at inria.fr

[2]Universitá degli studi di Padova, Dipartimento di Matematica Pura e applicata, Via Trieste 63, 35100 Padova, mzoppell at math.unipd.it

[1]http://bocop.org

- the relative orientations between successive links. For $i \in [2, \cdots, N]$, we note $\alpha_i = \theta_i - \theta_{i-1}$ the angle between the $(i-1)$-th and i-th links. The vector $(\alpha_2, \ldots, \alpha_N)$ defines the shape of the swimmer.

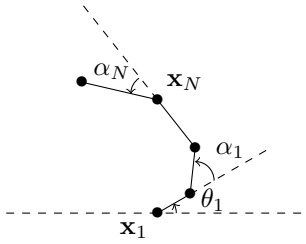

Fig. 1. Coordinates for the N-link swimmer.

B. Dynamics

We recall in this section the main steps to obtain the equations of motion using the Resistive Force Theory, as in [1]. The dynamics of the swimmer stems from Newton laws, neglecting the inertia:

$$\left\{ \begin{array}{l} \mathbf{F} = 0\,, \\ \mathbf{e}_z \cdot \mathbf{T}_{\mathbf{x}_1} = 0\,, \end{array} \right. \tag{2}$$

where $\mathbf{F}$ is the total force exerted on the swimmer by the fluid and $\mathbf{T}_{\mathbf{x}_1}$ is the total torque about the point $\mathbf{x}_1$.

The Resistive Force Theory uses the local drag approximation for the coupling between fluid and swimmer. We denote by s the arc length coordinate on the i-th link ($0 \leq s \leq L_i$) and by $\mathbf{v}_i(s)$ the velocity of the corresponding point. We also introduce the local frame $(\mathbf{e}_i, \mathbf{e}_i^\perp)$ defined by

$$\mathbf{e}_i = \begin{pmatrix} \cos(\theta_i) \\ \sin(\theta_i) \end{pmatrix} \quad \mathbf{e}_i^\perp = \begin{pmatrix} -\sin(\theta_i) \\ \cos(\theta_i) \end{pmatrix}$$

and write $\mathbf{x}_i(s) = \mathbf{x}_i + s\mathbf{e}_i$. By differentiation, we obtain,

$$\mathbf{v}_i(s) = \dot{\mathbf{x}}_i + s\ \dot{\theta}_i\ \mathbf{e}_i^\perp\,. \tag{3}$$

The force $\mathbf{f}_i$ acting on the i-th segment is assumed to depend linearly on the velocity. It is defined by

$$\mathbf{f}_i(s) := -\xi\left(\mathbf{v}_i(s)\cdot\mathbf{e}_i\right)\mathbf{e}_i - \eta\left(\mathbf{v}_i(s)\cdot\mathbf{e}_i^\perp\right)\mathbf{e}_i^\perp, \tag{4}$$

where ξ and η are the drag coefficients along the directions of $\mathbf{e}_i$ and $\mathbf{e}_i^\perp$. We thus obtain

$$\left\{ \begin{array}{l} \mathbf{F} = \displaystyle\sum_{i=1}^{N} \int_0^{L_i} \mathbf{f}_i(s)\, ds\,, \\ \mathbf{e}_z \cdot \mathbf{T}_{\mathbf{x}_1} = \mathbf{e}_z \cdot \displaystyle\sum_{i=1}^{N} \int_0^{L_i} \left(\mathbf{x}_i(s) - \mathbf{x}_1\right) \times \mathbf{f}_i(s)\, ds\,. \end{array} \right. \tag{5}$$

Using (3) and (4) into (5), the total force $\mathbf{F}$ is

$$-\sum_{i=1}^{N} L_i\xi(\dot{\mathbf{x}}_i\cdot\mathbf{e}_i)\,\mathbf{e}_i + \left(L_i\eta(\dot{\mathbf{x}}_i\cdot\mathbf{e}_i^\perp) + \frac{L_i^2}{2}\eta\dot{\theta}_i\right)\mathbf{e}_i^\perp\,, \tag{6}$$

and the total torque $\mathbf{e}_z \cdot \mathbf{T}_{\mathbf{x}_1}$ is

$$\begin{array}{l} -\displaystyle\sum_{i=1}^{N} \; L_i\eta\left(\dot{\mathbf{x}}_i\cdot\mathbf{e}_i^\perp\right)\,\left(\mathbf{x}_i - \mathbf{x}_1\right)\,\times\,\mathbf{e}_i^\perp + \\ \qquad L_i\xi\,\left(\dot{\mathbf{x}}_i\cdot\mathbf{e}_i\right)\,\left(\mathbf{x}_i - \mathbf{x}_1\right)\,\times\,\mathbf{e}_i\,+ \\ \qquad \frac{L_i^2}{2}\eta\dot{\theta}_i\quad\left(\mathbf{x}_i - \mathbf{x}_1\right)\,\times\,\mathbf{e}_i^\perp\quad + \\ \qquad \frac{L_i^2}{2}\,\eta\,\left(\dot{\mathbf{x}}_i\cdot\mathbf{e}_i^\perp\right)\;+\;\frac{L_i^3}{3}\,\eta\,\dot{\theta}_i\,. \end{array} \tag{7}$$

Differentiating (1) gives

$$\dot{\mathbf{x}}_i = \dot{\mathbf{x}}_1 + \sum_{k=1}^{i-1} L_k\dot{\theta}_k\mathbf{e}_k^\perp, \tag{8}$$

which is linear in $\dot{\mathbf{x}}_1 = (\dot{x}_1, \dot{y}_1)$ and the $(\dot{\theta}_k)$.

The angles $(\theta_k)_{2\leq k\leq N}$ are linear combinations of the $(\alpha_k)_{2\leq k\leq N}$, thus the expressions (6) and (7) are linear in $\dot{\mathbf{x}}_1$, $\dot{\theta}_1$ and $(\dot{\alpha}_k)_{2\leq k\leq N}$. As detailed in [1], the system (2) can therefore be rewritten in a matricial form by eliminating the $(\theta_k)_{2\leq k\leq N}$ and separating $(\dot{\mathbf{x}}_1, \dot{\theta}_1)$ from the $(\dot{\alpha}_k)_{2\leq k\leq N}$, leading to

$$\mathbf{A}(\theta_1, \alpha_2, \cdots, \alpha_N)\cdot\begin{pmatrix}\dot{\mathbf{x}}_1\\ \dot{\theta}_1\end{pmatrix} = \mathbf{B}(\theta_1, \cdots, \alpha_N)\cdot\begin{pmatrix}\dot{\alpha}_2\\ \vdots\\ \dot{\alpha}_N\end{pmatrix} \tag{9}$$

Matrix $\mathbf{A}$ is known as the "Grand Resistance Matrix" and is invertible (see [1]). We define the family of vector fields $\{\tilde{\mathbf{g}}\,(\theta_1, \alpha_2, \cdots, \alpha_N)\} := \mathbf{A}^{-1}\mathbf{B}$. Then the dynamics of the swimmer is finally expressed as

$$\begin{pmatrix}\dot{\alpha}_2\\ \vdots\\ \dot{\alpha}_N\\ \dot{\mathbf{x}}_1\\ \dot{\theta}_1\end{pmatrix} = \sum_{i=1}^{N-1}\begin{pmatrix}\mathbf{b}_i\\ \tilde{\mathbf{g}}_i\,(\theta_1, \alpha_2, \cdots, \alpha_N)\end{pmatrix}\dot{\alpha}_{i+1}\,. \tag{10}$$

where $\mathbf{b}_i$ is the $i-$th vector of the canonical basis of $\mathbf{R}^{N-1}$.

III. CONTROLLABILITY

This Section is devoted to the controllability of the N-link swimmer. We prove that there exist control functions which allow the swimmer to move everywhere in the plane.

Theorem 3.1: Consider the N-link swimmer described in Section II evolving in the space $\mathbf{R}^2$. Then for almost every lengths of the sticks $(L_i)_{i=1,\cdots,N}$ and for any initial configuration $(\mathbf{x}_1^i, \theta_1^i, \alpha_2^i, \cdots, \alpha_N^i) \in \mathbf{R}^2 \times [0, 2\pi]^N$, any final configuration $(\mathbf{x}_1^f, \theta_1^f, \alpha_2^f, \cdots, \alpha_N^f)$ and any final time $T > 0$, there exists a shape function $(\alpha_2, \cdots, \alpha_N) \in \mathcal{W}^{1,\infty}([0,T])$, satisfying $(\alpha_2, \cdots, \alpha_N)(0) = (\alpha_2^i, \cdots, \alpha_N^i)$ and $(\alpha_2, \cdots, \alpha_N)(T) = (\alpha_2^f, \cdots, \alpha_N^f)$ and such that if the self-propelled swimmer starts in position $(\mathbf{x}_1^i, \theta_1^i)$ with the shape $(\alpha_2^i, \cdots, \alpha_N^i)$ at time $t = 0$, it ends at position $(\mathbf{x}_1^f, \theta_1^f)$ and shape $(\alpha_2^f, \cdots, \alpha_N^f)$ at time $t = T$ by changing its shape along $(\alpha_2, \cdots, \alpha_N)(t)$.

Proof: The proof of the theorem is divided into three steps. First, we show the analyticity of the dynamics vector fields.

Then, we prove the controllability of the Purcell swimmer (3-link), using the Chow theorem and the Orbit theorem. Finally, we generalize the result to the N-link swimmer.

A. Regularity

We first prove that the vector fields $(\tilde{\mathbf{g}}_i)$ are analytic on $\mathcal{M}$. From (6) and (7), $\mathbf{A}$ and $\mathbf{B}$ belong to the set of matrices whose entries are analytic functions on $[0,2\pi]^N$. Since the coefficients of $\mathbf{A}^{-1}$ are obtained by multiplication and division of those of $\mathbf{A}$, and because $det(\mathbf{A}) \neq 0$, the entries of $\mathbf{A}^{-1}$ remain analytic functions on $[0,2\pi]^N$. Thus, the $(\tilde{\mathbf{g}}_i)_{i=1,\cdots,N} := \mathbf{A}^{-1}\mathbf{B}$ are analytic on $[0,2\pi]^N$.

B. Controllability of the Purcell Swimmer (N=3)

Taking $N = 3$ in (10) gives the dynamics

$$\begin{pmatrix} \dot{\alpha}_2 \\ \dot{\alpha}_3 \\ \dot{x}_1 \\ \dot{y}_1 \\ \dot{\theta}_1 \end{pmatrix} = \mathbf{g}_1(\theta_1,\alpha_2,\alpha_3)\dot{\alpha}_2 + \mathbf{g}_2(\theta_1,\alpha_2,\alpha_3)\dot{\alpha}_3\,. \qquad (11)$$

We now express the Lie algebra of the vector fields $\mathbf{g}_1$ and $\mathbf{g}_2$ for any $\theta_1 \in [0,2\pi]$ at $(\alpha_2,\alpha_3) = (0,0)$, for a swimmer whose sticks have the length $L_1 = L_3 = L$ and $L_2 = 2L$ where $L > 0$. First we have

$$\mathbf{g}_1\,(\,\theta_1,0,0\,) = \begin{pmatrix} 1 \\ 0 \\ \frac{9L\sin(\theta_1)}{64} \\ -\frac{9L\cos(\theta_1)}{64} \\ \frac{27}{32} \end{pmatrix}, \quad \mathbf{g}_2\,(\theta_1,0,0) = \begin{pmatrix} 0 \\ 1 \\ -\frac{7L\sin(\theta_1)}{64} \\ \frac{7L\cos(\theta_1)}{64} \\ -\frac{5}{32} \end{pmatrix}$$

Then, the iterated Lie brackets are equals to

$$[\mathbf{g}_1,\mathbf{g}_2](\theta_1,0,0) = \left(0,0,\frac{7L(\eta-\xi)\cos(\theta_1)}{128\xi},\frac{7L(\eta-\xi)\sin(\theta_1)}{128\xi},0\right)^T,$$

$$[\mathbf{g}_1,[\mathbf{g}_1,\mathbf{g}_2]](\theta_1,0,0) = \begin{pmatrix} 0 \\ 0 \\ -\frac{L\left(126\eta^2+31\xi\eta-76\xi^2\right)\sin(\theta_1)}{4096\eta\xi} \\ \frac{L\left(126\eta^2+31\xi\eta-76\xi^2\right)\cos(\theta_1)}{4096\eta\xi} \\ -\frac{3\left(9\eta^2-4\xi\eta+4\xi^2\right)}{2048\eta\xi} \end{pmatrix},$$

$$[\mathbf{g}_2,[\mathbf{g}_1,\mathbf{g}_2]](\theta_1,0,0) = \begin{pmatrix} 0 \\ 0 \\ \frac{L\left(36\eta^2-103\xi\eta+148\xi^2\right)\sin(\theta_1)}{4096\eta\xi} \\ -\frac{L\left(36\eta^2-103\xi\eta+148\xi^2\right)\cos(\theta_1)}{4096\eta\xi} \\ \frac{3\left(9\eta^2-4\xi\eta+4\xi^2\right)}{2048\eta\xi} \end{pmatrix}.$$

The determinant of the matrix whose columns are the 5 previous vector fields is equal to

$$\frac{21L^2(\eta-\xi)^2(45\eta+112\xi)\left(9\eta^2-4\eta\xi+4\xi^2\right)}{536870912\eta^2\xi^3}\,. \qquad (12)$$

Since the drag coefficients ξ and η are positive, this determinant is null only when $\xi = \eta$. This would indicate an isotropic drag, as we would have for spheres instead of sticks. Thus in our case the Lie algebra of the vector fields $\mathbf{g}_1$ and $\mathbf{g}_2$ is fully generated at the point $(\theta_1,0,0)$, for any $\theta_1 \in [0,2\pi]$.

Remark that any point $(\alpha_2,\alpha_3,\mathbf{x}_1,\theta_1) \in [0,2\pi]^2 \times \mathbf{R}^2 \times [0,2\pi]$ belongs to the orbit of the point $(0,0,\mathbf{x}_1,\theta_1)$. Since the vector fields are analytic, the Orbit Theorem ([13]) states that the Lie algebra of $\mathbf{g}_1$ and $\mathbf{g}_2$ is fully generated everywhere in the manifold $[0,2\pi]^2 \times \mathbf{R}^2 \times [0,2\pi]$.

To conclude, by Chow Theorem ([9]) we get the controllability of the Purcell swimmer.

C. Controllability of the N-link swimmer

The third step is to generalize the controllability result to the N-link swimmer, whose dynamics is described by (10). By construction, the vector fields $\mathbf{g}_i$ generate the tangent space of the manifolds $[0,2\pi]^{N-1}$,

$$\text{Span}(\mathbf{g}_1,\cdots,\mathbf{g}_{N-1}) = \mathbf{R}^{N-1}\,. \qquad (13)$$

The two vector fields $\mathbf{g}_1$ and $\mathbf{g}_2$ are related to the Purcell's one defined in (11): we add $N-2$ rows of zeroes, take sticks of null length $L_i = 0$ for $4 \leq i \leq N-1$, while keeping the three sticks $L_1 = L_3 = L$ and $L_2 = 2L$.

In this case, for any $(\mathbf{x}_1,\theta_1) \in \mathbf{R}^2 \times [0,2\pi]$, III-B shows that $\mathbf{g}_1(\theta_1,0,\cdots 0)$, $\mathbf{g}_2(\theta_1,0,\cdots 0)$ and their iterated Lie brackets $[\mathbf{g}_1,\mathbf{g}_2](\theta_1,0,\cdots 0)$, $[\mathbf{g}_1,[\mathbf{g}_1,\mathbf{g}_2]](\theta_1,0,\cdots 0)$, and $[\mathbf{g}_2,[\mathbf{g}_1,\mathbf{g}_2]](\theta_1,0,\cdots 0)$ are linearly independent.

Therefore, the Lie algebra of the family $(\mathbf{g}_i)_{i=1,\cdots,N-1}$ at the point $(\theta_1,0,\cdots,0)$ is equal to the tangent space $T_{(0,\cdots,0,\mathbf{x}_1,\theta_1)}\mathcal{M}$. Then, by analyticity of the vector fields $\mathbf{g}_i$, the Orbit Theorem states that the Lie algebra is fully generated everywhere for a swimmer whose the length of sticks verify $L_1 = L_3 = L$, $L_2 = 2L$ and $L_{i\geq 4} = 0$.

We define by $D^{(0,\cdots,0)}$, the function that maps $(L_1,\cdots,L_N)$ to the determinant of the vectors $\mathbf{g}_1,\cdots,\mathbf{g}_{N-1}$ and their iterated Lie brakets at the point $(0,\cdots,0)$. Since the vector fields $\mathbf{g}_i$ depend analytically on the sticks length L_i, we get the analyticity of the function $D^{(0,\cdots,0)}$. Thus for any $L > 0$, the value of $D^{(0,\cdots,0)}$ at the point $(L,2L,L,0\cdots 0)$ is not null. By analyticity, it remains non null almost everywhere in $\mathbf{R}^N$. Therefore, we obtain that the Lie algebra is of full rank for almost every swimmer.

Finally, Chow Theorem gives the controllability in Th 3.1.

IV. MINIMUM TIME OPTIMAL CONTROL PROBLEM FOR THE N-LINK SWIMMER

We present in IV-A the minimum time optimal control problem for the N-link swimmer, which is well defined from the controllability result proven in III. Then in IV-B we present the numerical method used to solve this problem.

A. Minimum Time Problem

For any time $t > 0$, we denote the state of the swimmer by $\mathbf{z}(t) := (\alpha_2, \cdots, \alpha_N, \mathbf{x}_1, \theta_1)(t)$, the control function by $\mathbf{u}(t) := (\dot{\alpha}_2, \cdots, \dot{\alpha}_N)(t)$ and the dynamics by $\mathbf{f}(\mathbf{z}(t), \mathbf{u}(t)) = \sum_{i=1}^{N-1} \mathbf{g}_i(\mathbf{z}(t))\, \dot{\alpha}_{i+1}(t)$.

We now assume that the swimmer starts at the initial configuration $\mathbf{z}^i$, and we set a final state $\mathbf{z}^f$. We want to find a swimming strategy that minimizes the time to reach the final configuration, i.e.,

$$(OCP) \begin{cases} \inf\ t_f\,, \\ \dot{\mathbf{z}}(t) = f(\mathbf{z}(t), \mathbf{u}(t))\ ,\ \forall t \in [0, t_f]\,, \\ \mathbf{u}(t) \in \mathbf{U} := [-1, 1]^N\ ,\ \forall t \in [0, t_f]\,, \\ \mathbf{z}(0) = \mathbf{z}^i \quad ,\quad \mathbf{z}(t_f) = \mathbf{z}^f\,. \end{cases}$$

By applying Filippov-Cesary Theorem ([21]), there exists a minimal time such that the constraints are satisfied i.e., the infimum can be written as a minimum.

B. Numerical Optimization

In order to solve this optimal control problem, we use a so-called direct approach. The direct approach transforms the infinite dimensional optimal control problem (OCP) into a finite dimensional optimization problem (NLP). This is done by a discretization in time applied to the state and control variables, as well as the dynamics equation. These methods are usually less precise than indirect methods based on Pontryagin's Maximum Principle, but more robust with respect to the initialization. Also, they are more straightforward to apply, hence they are widely used in industrial applications.

Summary of the time discretization:

$t \in [0, tf]$	$\rightarrow$	$\{t_0 = 0, \ldots, t_N = tf\}$
$z(\cdot), u(\cdot)$	$\rightarrow$	$X = \{z_0, \ldots, z_N, u_0, \ldots, u_{N-1}, tf\}$
$Criterion$	$\rightarrow$	$\min\ tf$
$Dynamics$	$\rightarrow$	$(ex : Euler)\ z_{i+i} = z_i + hf(z_i, u_i)$
$Controls$	$\rightarrow$	$-1 \leq u_i \leq 1$
$I/F\ Cond.$	$\rightarrow$	$\Phi(z_0, z_N) = 0$

We therefore obtain a nonlinear programming problem on the discretized state and control variables

$$(NLP) \begin{cases} \min\ F(X) = tf \\ LB \leq C(X) \leq UB \end{cases}$$

All tests were run using the software BOCOP ([7]). The discretized nonlinear optimization problem is solved by the well-known solver IPOPT [22] with MUMPS [5], while the derivatives are computed by sparse automatic differentiation with ADOL-C [23] and COLPACK [11]. In the numerical experiments, we used a Midpoint (implicit 2nd order) discretization with 1000 time steps. Execution times on a Xeon 3.2GHz CPU were a few minutes.

V. NUMERICAL SIMULATIONS FOR THE PURCELL'S SWIMMER (N= 3)

We present here the numerical simulations for the Purcell swimmer (3 sticks). Without making any assumptions on the structure of the optimal trajectory, we obtain a solution with periodic strokes. We compare this stroke to the one of Purcell ([18], [6]), and observe that it gives a better displacement speed.

In the rest of the paper, we match the notations used in [6], and denote the state of the swimmer (see Fig 2) by

- the position (x_2, y_2) of the center of the second stick, and its angle with the x-axis $\theta_2 := \theta_1 - \alpha_2$.
- the shape angles $\beta_1 := -\alpha_2$ and $\beta_3 := \alpha_3$.

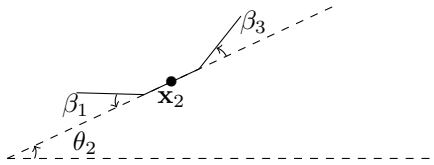

Fig. 2. Purcell's 3-link swimmer.

This reformulation gives the new dynamics

$$\begin{pmatrix} \dot{\beta}_1 \\ \dot{\beta}_3 \\ \dot{\mathbf{x}}_2 \\ \dot{\theta}_2 \end{pmatrix} = \mathbf{M}\,(\theta_2, \beta_1) \begin{pmatrix} \dot{\alpha}_2 \\ \dot{\alpha}_3 \\ \dot{\mathbf{x}}_1 \\ \dot{\theta}_1 \end{pmatrix}\ ,$$

$$\mathbf{M}\,(\theta_2, \beta_1) = \begin{pmatrix} -1 & 0\,0\,0 & 0 \\ 0 & 1\,0\,0 & 0 \\ \sin(\theta_2)+\cos(\beta_1) & 0\,1\,0 & -\sin(\theta_2) \\ -\cos(\beta_1)-\cos(\theta_2) & 0\,0\,1 & \cos(\theta_2) \\ -1 & 0\,0\,0 & 1 \end{pmatrix}\ .$$

As a result, the dynamics (10) reads in this case

$$\begin{pmatrix} \dot{\beta}_1 \\ \dot{\beta}_3 \\ \dot{\mathbf{x}}_2 \\ \dot{\theta}_2 \end{pmatrix} = \tilde{\mathbf{f}}_1\,(\theta_2, \beta_2, \beta_3)\ \dot{\beta}_1 + \tilde{\mathbf{f}}_2\,(\theta_2, \beta_2, \beta_3)\ \dot{\beta}_3 \qquad (14)$$

where for $i = 1, 2$

$$\tilde{\mathbf{f}}_i\,(\theta_2, \beta_1, \beta_3) = \mathbf{M}\,(\theta_2, \beta_1,)\,\tilde{\mathbf{g}}_i\,(\theta_1, \alpha_2, \alpha_3)\ . \qquad (15)$$

Since the new state variables are the image of the former ones by a one-to-one mapping, the controllability result in Section III-B also holds for (14).

A. The classical Purcell stroke

We recall the stroke presented by Purcell in [18] in order to compare it to the optimal strategy given by our numerical results. Let us denote by $\Delta\theta$ the angular excursion, meaning that β_1 and β_3 belong to $[-\frac{\Delta\theta}{2}, \frac{\Delta\theta}{2}]$. The Purcell stroke is defined by the periodic cycle of deformation over $[0, T]$:

$$\big(\,\beta_1(t), \beta_3(t)\,\big) = \begin{cases} \big(\,\frac{4\Delta\theta}{T}t - \frac{\Delta\theta}{2}, \frac{\Delta\theta}{2}\,\big) & \text{if } 0 \leq t \leq \frac{T}{4} \\ \big(\,\frac{\Delta\theta}{2}, -\frac{4\Delta\theta}{T}t + \frac{3\Delta\theta}{2}\,\big) & \text{if } \frac{T}{4} \leq t \leq \frac{T}{2} \\ \big(-\frac{4\Delta\theta}{T}t + \frac{5\Delta\theta}{2}, -\frac{\Delta\theta}{2}\,\big) & \text{if } \frac{T}{2} \leq t \leq \frac{3T}{4} \\ \big(-\frac{\Delta\theta}{2}, \frac{4\Delta\theta}{T}t - \frac{7\Delta\theta}{2}\,\big) & \text{if } \frac{3T}{4} \leq t \leq T \end{cases}\ .$$

In the following, we call the "classical" Purcell stroke the one corresponding to $\Delta\theta = \frac{\pi}{3}$, with $T = 4\Delta\theta$ chosen to satisfy the constraints on the speed of deformation stated in (OCP), i.e., $u_i(t) := \dot{\beta}_i(t) \in [-1, 1]$.

B. Comparison of the optimal stroke and Purcell stroke

We set the initial position $\mathbf{x}_2, \theta_2 = (0, 0, 0)$ and the final position $\mathbf{x}_2, \theta_2 = (-0.25, 0, 0)$. We also constrain the angles β_1 and β_3 in $[-\frac{\pi}{6}, \frac{\pi}{6}]$ for all time. Solving the minimum time problem with the direct method gives us a solution that is actually periodic, as shown on Fig. 3. We observe that he x-displacement is not monotonous: during each stroke, the swimmer alternately swims forward, closer to the target, and goes partially backward.

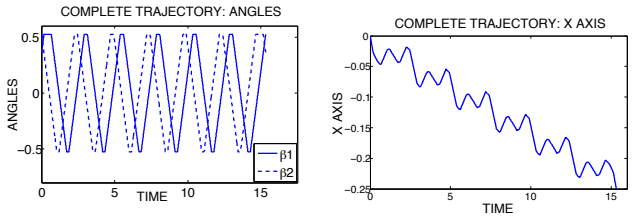

Fig. 3. Angles and x-displacement for a whole periodic trajectory.

Now we extract one stroke from this solution, and compare it with the Purcell stroke. We show on Fig. 4 the angles functions β_1 and β_3, as well as the phase portrait. The scale for the angles is inverted on the optimal stroke for a better comparison with the Purcell stroke. Note that the time required to complete our candidate for an optimal stroke is shorter than for the Purcell one (roughly 2.81 versus 4.19). We illustrate on Fig. V-B the shape changes in the (X,Y) plane for the Purcell and optimal stroke.

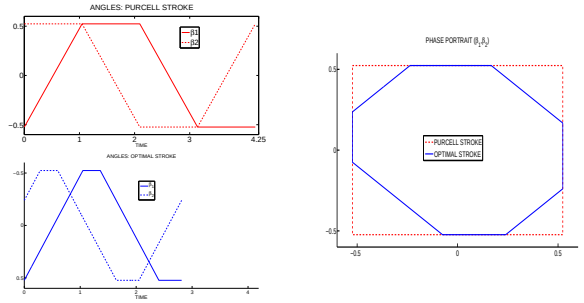

Fig. 4. Angles and phase portrait - Purcell stroke and optimal stroke.

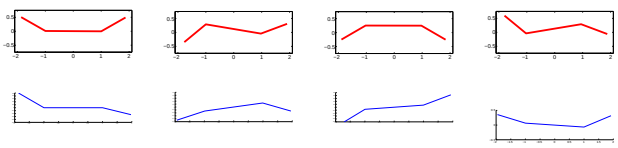

Fig. 5. Purcell and optimal stroke at $t = 0, T/4, T/2, 3T/4$

Fig. 6 shows the $x-$displacement of the swimmer with the classical Purcell stroke (dashed) and the optimal stroke (solid). Both trajectories were recomputed in Matlab using the same ODE solver, and the results for the Purcell stroke match the ones in [6]. The final time $t_f = 15.3252$ is the one given by the numeric simulation to reach $\mathbf{x}_2 = (-0.25\,, 0)$. We see that using Purcell strokes, the swimmer only reaches $(\approx -0.18, 0)$, which confirms that our optimal stroke allows a greate x-displacement.

More precisely, each optimal stroke gives a $x-$displacement close to the Purcell stroke, however the cycle of deformation is performed in less time. Therefore, for a given time frame, more optimal strokes can be performed, leading to an overall greater displacement. In Fig. 6, almost 3.5 Purcell strokes are performed, while 6 optimal strokes are completed within the same time.

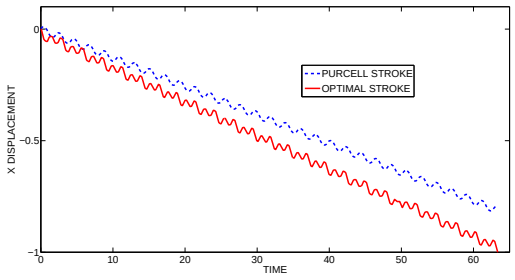

Fig. 6. x and y displacement for one Purcell and one optimal stroke.

Remark: The initial shape of the swimmer is not identical for both strategies, however the increasing gap between the two curves clearly shows that the optimal stroke is faster.

We study now for both strokes the x-displacement for one stroke with respect to the angular excursion, as shown on Fig. 7. In both cases, we see that a larger interval of angular excursion gives a greater displacement. We also observe on Tab. I that the optimal stroke consistently gives a speed better by 15% than the Purcell stroke for angular excursions below $\pi/3$. The increasing gap for greater angular excursions may be a limitation of the RFT

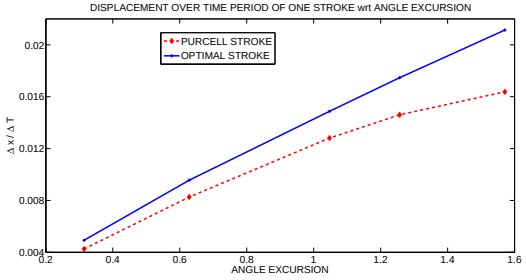

Fig. 7. Δ_x/T (x-displacement for one stroke divided by stroke period), wrt angular excursion for Purcell and optimal strokes.

Δ_θ	$\pi/10$	$\pi/5$	$\pi/3$	$2\pi/5$	$\pi/2$
Δ_x/T (Purcell)	4.257E-3	8.262E-3	1.281E-2	1.461E-2	1.638E-2
Δ_x/T (optimal)	4.927E-3	9.563E-3	1.487E-2	1.747E-2	2.114E-2
Speed gain	15.74%	15.74%	16.12%	19.59%	29.09%

TABLE I

GAIN BETWEEN PURCELL AND OPTIMAL STROKES, FOR DIFFERENT ANGULAR EXCURSIONS.

VI. CONCLUSIONS

In this paper we study the N-link swimmer, and use the Resistive Force Theory to derive its dynamics, as was done in [1]. In this context, we prove that for N greater than 3 and for almost any N-uplet of sticks lengths, the swimmer is globally controllable in the whole plane. Then, we focus on finding a swimming strategy that leads the N-link swimmer from an fixed initial position to a given final position, in minimum time. As a consequence of the controllability result, we show that there exists a shape change function which allows to reach the final state in a minimal time. We formulate this optimal control problem and solve it with a direct approach (BOCOP) for the case $N = 3$ (Purcell swimmer). Without any assumption on the structure of the trajectory, we obtain a periodic solution, from which we identify an optimal stroke. Comparing this optimal stroke with the Purcell one confirms that it is better, actually giving a greater displacement speed. More precisely, the difference is due to the fact that optimal stroke is executed in less time than the Purcell one.

Current and still ongoing works include solving the optimal control problem for more complex displacements (along the y axis, rotations) and/or for different cost functions, such as energy dissipation. Also, noticing that the N-link swimmer was introduced in [1] in the perspective of approximating the motion of several living micro-organisms, an interesting extension of this model is to generalize the simulations to greater values of N, and try to compare the results with biological data. Another interesting direction is to study formally the existence of the periodic solution for the optimal control problem.

REFERENCES

[1] F. Alouges, A. DeSimone, L. Giraldi, and M. Zoppello. Self-propulsion of slender micro-swimmers by curvature control: N-link swimmers. *accepted in International Journal of Non-Linear Mechanics*, 2013.

[2] F. Alouges, A. Desimone, L. Heltai, A. Lefebvre, and B. Merlet. Optimally swimming stokesian robots. *DCDS-B*, 2013.

[3] F. Alouges, A. DeSimone and A. Lefebvre. Optimal strokes for low Reynolds number swimmers: an example. *Journal of Nonlinear Science*, 2008.

[4] F. Alouges, and L. Giraldi. Enhanced controllability of low Reynolds number swimmers in the presence of a wall. *Acta Applicandae Mathematicae*, April 2013.

[5] P. R. Amestoy, I. S. Duff, J. Koster, and J-Y. LÉxcellent. A fully asynchronous multifrontal solver using distributed dynamic scheduling. *SIAM Journal of Matrix Analysis and Applications*, 23(1):15–41, 2001.

[6] L. E. Becker, S. A. Koehler, and H. A. Stone. On self-propulsion of micro-machines at low Reynolds number: Purcell's three-link swimmer. *J. Fluid Mech.*, 2003.

[7] F. Bonnans, P. Martinon, and V. Grélard. Bocop - A collection of examples. Technical report RR-8053, INRIA, 2012.

[8] T. Chambrion and A. Munnier. Generic controllability of 3d swimmers in a perfect fluid. *SIAM Journal on Control and Optimization, 50(5):28142835*, 2012.

[9] J. M. Coron. *Control and Nonlinearity*. American Mathematical Society, 2007.

[10] B. M. Friedrich, I. H. Riedel-Kruse, J. Howard, and F. Jülicher. High-precision tracking of sperm swimming fine structure provides strong test of resistive force theory. *The Journal of Experiment Biology*, 2010.

[11] A. Gebremedhin, A. Pothen, and A. Walther. Exploiting sparsity in jacobian computation via coloring and automatic differentiation: a case study in a simulated moving bed process. In C. Bischof et al, editor, *Lecture Notes in Computational Science and Engineering 64*, pages 339–349. Springer, 2008. Proceedings of the Fifth International Conference on Automatic Differentiation (AD2008).

[12] J. Gray and J. Hancock. The propulsion of sea-urchin spermatozoa. *Journal of Experimental Biology*, 1955.

[13] V. Jurdjevic. *Geometric control theory*. Cambridge University Press., 1997.

[14] E. Lauga, T. Powers. The hydrodynamics of swimming micro-organisms. *Rep. Prog. Phys. 72, 096601*, 2009.

[15] J. Lohéac, J. F. Scheid, and M. Tucsnak. Controllability and time optimal control for low Reynolds numbers swimmers. Acta Appl. Math., 123(1):175-200, 2013.

[16] R. Montgomery. *A tour of subriemannian geometries, their geodesics and applications.* AMS, Providence, 2002.

[17] E. Passov, and Y. Or. *Dynamics of Purcell's three-link microswimmer with a passive elastic tail.* European Physical Journal E 35:78, 2012.

[18] E. M. Purcell. Life at low Reynolds number. *American Journel of Physics*, 45:3–11, 1977.

[19] D. Tam and A. E. Hosoi. Optimal strokes patterns for purcell's three link swimmer. *Physical Review Letters*, 2007.

[20] G. Taylor. Analysis of the swimming of microscopic organisms. *Proc. R. Soc. Lond. A*, 209:447–461, 1951.

[21] E. Trelat. *Contrôle optimal : théorie and applications.* Vuibert, Collection Mathématiques Concrètes, 2005.

[22] A. Wächter and L.T. Biegler. On the implementation of a primal-dual interior point filter line search algorithm for large-scale nonlinear programming. *Mathematical Programming*, 106(1):25–57, 2006.

[23] A. Walther and A. Griewank. Getting started with Adol-c. In U. Naumann and O. Schenk, editors, *Combinatorial Scientific Computing*. Chapman-Hall CRC Computational Science, 2012.